Synchronization by Disorder in Coupled Systems

Normand Mousseau

Theoretical Physics, University of Oxford, 1 Keble Road, Oxford, OX1 3NP, United Kingdom
and Département de Physique and Groupe de Recherche en Physique et Technologie des Couches Minces,
*Université de Montréal, C.P. 6128 Succ. Centre-ville, Montréal (Québec), Canada H3C 3J7**

Effects of quenched disorder on a coupled map model of earthquakes are studied. In its original version, this model is known to display a self-organized critical distribution of avalanches. However, when some finite amount of quenched disorder is introduced, the bulk sites synchronize fully and a single stable system-wide avalanche appears. This synchronization is found for a wide band of disorder and goes against some recent predictions about integrate-and-fire models. [S0031-9007(96)00780-6]

Effects of disorder on dynamical systems remain only partially understood. In some cases, introduction of disorder is known to destroy the correlations already built up [1]. In others, when present at small doses, it does not play any significant role [2,3]. More interesting are effects like stochastic resonance which go against common expectation: Some chaotic systems can find their signal-to-noise ratio increased with increasing noise [4]. This has also been seen, for example, in coupled Ginzburg-Landau equations [5] and in totalistic cellular automata [6], where noise diminishes slightly the chaotic situation and in Lorenz systems where noise creates a stabilization of the flip-flop process [7]. Recently, Tsodyks, Mitkov, and Sompolinsky [1] proposed that the effects of noise or disorder on coupled dynamical systems should be strongly determined by the generic type of rule defining the evolution in these models. From a mean-field solution, they speculated that for integrate-and-fire (IAF) neuron models, which are characterized by discontinuous rules, disorder should always destroy immediately all synchronization contrary to what is seen in coupled maps with continuous dependence [2]. However, Bottani [3] showed that for some mean-field IAF models *phase locking* synchronization, where all sites maintain their phase with respect to the others, could survive small amounts of frozen disorder. In this Letter, I present a specific example of an IAF coupled-map rule where the introduction of disorder causes an uncorrelated system to fully synchronize in the sense that all bulk sites fire *at the same time*, an effect stronger than phase locking and much more dramatic than what is customarily found with stochastic resonance. The rule retained was first proposed by Olami, Feder, and Christensen (OFC) as a model for earthquakes and is known to display, in the absence of frozen disorder, a self-organized-critical (SOC) distribution of avalanches. For some region of the parameters, the SOC phase survives the introduction of a small albeit finite amount of quenched disorder. Past a finite threshold, the system becomes fully synchronized. This phase exists for the full range of parameters tested and a finite range of disorder. As the disorder increases

the coupled map becomes SOC again before showing an exponential decay in the distributions.

The discovery of self-organized criticality in nonconservative coupled-map models of earthquakes has attracted a lot of attention to models like the one used here since it was first shown to exist [8]. Similar non-mean-field coupled maps have also been applied to biological problems such as firing neurons [9]. In this latter case, the interest does not lie in the SOC distribution but rather in the phase locking and the speed of convergence between local events. Coupled maps are mathematical objects where each site can take a value from a continuum and evolve following an often complex function of the site itself and its local neighbors. These objects are therefore ideal to describe coupled macroscopic systems like fireflies, hearth cells, or neurons where each individual evolves in time following a nontrivial function of its own state and environment. In the earthquake model, proposed by Olami, Feder, and Christensen [8] and studied in details by Grassberger [10] and Middleton and Tang [11], each site or map represents a block moving along some direction under the push of a field but connected, via nonlinear forces, to its first neighbors. In neural terminology, a single site represents a neuron, affected by both global loading and the signals regularly received by and sent to its firing neighbors [9].

Recent studies of these models have focused on homogeneous lattices with or without periodic boundary conditions. But it is clear that the real systems modeled by these objects are not homogeneous. In a geological fault, for example, the local friction between the moving plates, which influences both the rate of motion and the redistribution on the neighbors in the OFC model, cannot be expected to be a constant value but should fluctuate according to local variations. Similarly, the local elasticity of the sheets, which determines how the energy is transferred from one point to another, is also expected to be variable. A first step is therefore to simply see how the introduction of quenched disorder in the simple coupled-map representation for these systems will affect their dynamical behavior. Some work has already been done along these lines. Jánosi and Kertész [12] studied the influence of

randomness in the threshold for the OFC rule and found that this type of disorder destroys criticality and changes the distribution of avalanche size from power law to exponential. Ceva [13], for his part, looked at uncorrelated and correlated disorder in the redistribution parameter α. He was interested, however, in the effects of concentration of defects and not their amplitude. He found, in this case, that SOC is stable under small concentration of defects.

A full description of the OFC model and its properties can be found in many papers (see, for example, [8] and [10]) and will be described only succinctly here. A continuous function $F_i(t)$ is assigned to every site of a square lattice. Each function evolves linearly in time following $dF_i(t)/dt = 1$. When a site, say, i reaches a threshold value $\tau_C (= 1$ in this paper), time evolution is stopped and an event is triggered: (1) The function is set back to zero, $F_i(t) \rightarrow F_i't = 0$, and (2) a certain weight is redistributed to the neighboring sites j, $F_j(t) \rightarrow F_j'(t) = F_j(t) + \Delta_i(t)$, where $\Delta_i(t) = \alpha_i F_i(t)$. This process is repeated until all functions fall below threshold. The number of sites which have been triggered gives the size of the avalanche. Time evolution is then restarted until another site hits the threshold. In the present work, disorder is introduced in the redistribution fraction α_i which now varies from site to site as $\alpha_i = \alpha + \delta_i$, where δ_i is a random number taken from a linear distribution $[-\delta, \delta]$. In order to make sure that no site, once the disorder is added to α, becomes an effective source in the lattice or reaches the conservative regime, I have limited my investigations to cases where $0 < \alpha_i < 0.25$. The disorder is quenched in *before* the start of the simulation. At $t = 0$, the state of the system, $[F_i]$, is also chosen randomly from a linear distribution $[0, 1]$. This ensures than two sites cannot act simultaneously as seeds for an event.

The propagation of the avalanche is done radially from the first toppled site. Physically, this presupposes that the triggering time is much faster than the propagation time. The exact type of propagation plays an important role in determining the dynamical behavior, especially in the presence of open boundaries, as is the case for the model studied. Results obtained with other types of propagation will be discussed elsewhere [14]. The program used here implements the Grassberger algorithm which improves enormously the efficiency over a straightforward application of the algorithm (see [10] for details).

As can be seen in Fig. 1, the introduction of quenched disorder can affect qualitatively the dynamical behavior of the OFC model. For $\alpha \geq \alpha_d \approx 0.10$, the lattice continues to demonstrate a SOC distribution of avalanches (Fig. 2) even for some finite presence of quenched disorder. Size effects are noticeable in this phase, and the exponent in the power-law distribution has to be rescaled by a factor of the form $1 - 1/L^{\nu}$, where ν has been found to be 0.10. Below α_d, the system synchronizes with any amount of disorder although the transient period towards a fully synchronized state can be extremely long. The dynamical behavior of the perfect OFC model also depends upon
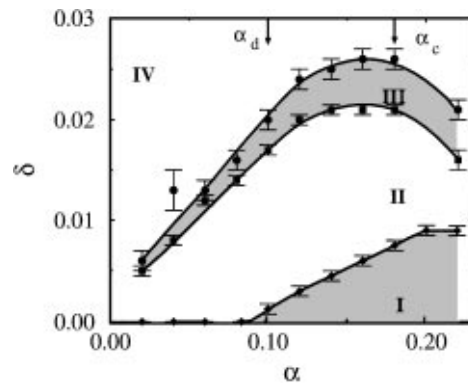

FIG. 1. Approximate phase diagram for the OFC model as a function of the redistribution factor α and the quenched disorder δ. The points result from simulations on a 100×100 lattice. The phases are discussed in the text. The arrow at $\alpha = 0.10$ indicates the position of α_d and the one at $\alpha = 0.18$ indicates α_c.

α. In an extensive study of the OFC model, Grassberger [10] showed that, although the transition at very small α's reported by Olami *et al.* was only due to the limited size of the original simulations, something happened at $\alpha_c \approx 0.18$. For $\alpha < \alpha_c$, large avalanches happen mainly near the surface. Deep in the bulk, there is complete phase locking, i.e., all sites fall one at a time but within the same period; there is no global synchronization. When $\alpha > \alpha_c$, large avalanches appear everywhere, from the surface to deep inside the lattice. A SOC distribution holds, however, for all values of α's. The fact that $\alpha_c \neq \alpha_d$ indicates that the mechanism which controls synchronization is somewhat different from the one which allows propagation of large avalanches from the edges in the perfect SOC.

So, for $\alpha > \alpha_d$, the transition from phase I (SOC distribution) to II (synchronized) happens only for a finite δ. Moreover, this disorder-to-order transition is clear and sharp, except for large α's (close to 0.25) where the
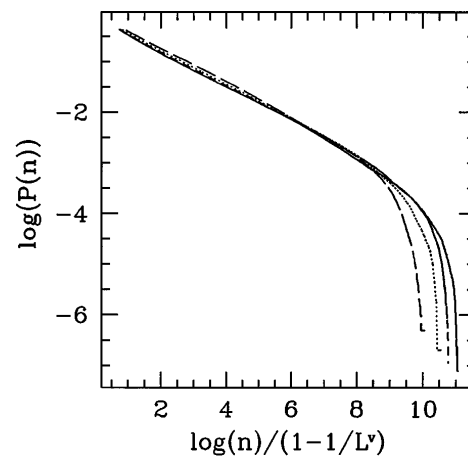

FIG. 2. Integrated probability distribution for avalanches as a function of their size, n, for lattices in phase I of Fig. 1. $\alpha = 0.18$ and $\delta = 0.002$. Lattice sizes are $L = 49$ (long dashes), 100 (dots), 169 (short dashes), and 225 (solid line). The exponent $\nu = 0.10$.

exact position of the transition between SOC and synchronized phases becomes slightly blurred. As mentioned before, from the initial random configuration, the transient in phase II from the initial random configuration to full synchronization of phase II can be relatively long. In Fig. 3, we see that all avalanches are slowly absorbed into a single one which ends up dominating almost the whole lattice. For the chosen parameters in Fig. 3, the main avalanche involves almost 90% of all the sites and, although slightly fluctuating, remains remarkably stable. Looking at snapshots of this realization (Fig. 4), before and after a large avalanche has been triggered, we see that the 10% of sites not participating in it are situated at the edges of the lattice, the bulk region being perfectly synchronized. The boundaries between the bulk and edge regions, however, are not frozen and contribute to the fluctuations seen in Fig. 3. Edge sites themselves do not synchronize at all, and avalanches in this region are essentially of size one. When disorder becomes large enough, the system loses synchronization and falls back into a SOC distribution [phase III and Fig. 5(a)]. Here again, the transition is quite sharp and well defined. Because the largest avalanches do not reach a significant fraction of the system size, size effect seems to be much less important than in phase I. Finally, as quenched disorder is increased to a higher level, this SOC distribution makes a place for an exponential-like one [phase IV and Fig. 5(b)]. The transition from phase III to phase IV is relatively smooth and difficult to find precisely. As seen in Fig. 5(b), the distribution is not exactly exponential, except for the tail, but it decays much faster than a power law. In both these two phases, large avalanches become rare and never reach much more than a few tenths of the total size of the system, a proportion decreasing with increasing quenched disorder.
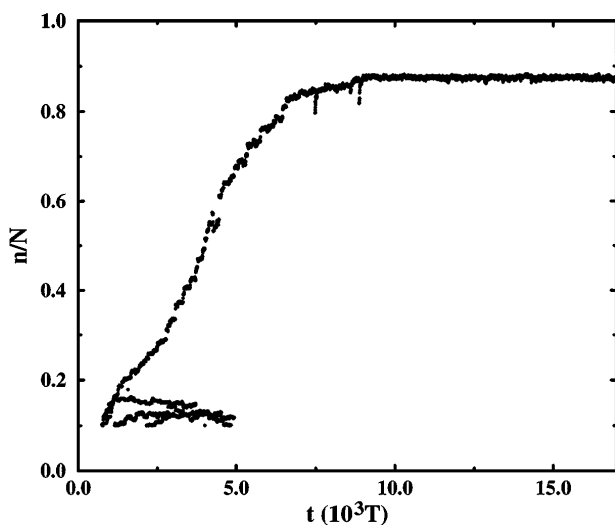
As mentioned in [10], in the absence of noise, the OFC rule on a lattice with periodic boundary conditions (PBC) does not display any collective mode: Sites are phase locked and triggered one at a time in a given order fixed from the first instant of simulation. When very small amounts of disorder are introduced, a distribution in the size of avalanche forms. But the decay of this distribution with size remains extremely fast, essentially exponential, and accelerates with increasing levels of disorder, so that the introduction of disorder does not change the qualitative behavior of the OFC rule when placed on a lattice with periodic boundary conditions. With or without disorder, open boundaries are needed to achieve collective modes. All results presented here were obtained on lattices with open boundaries on the four sides of a square lattice.

The unit of time retained in Figs. 2 and 3 is the period of return for avalanches on a lattice with periodic boundary condition, $P = 1 - 4\alpha$ [9]. The synchronized phase displays a characteristic time closely related to this one and independent of the period associated with the edge sites. This is somewhat surprising and contrary to what would be expected based on the behavior of the closely related earthquake model of Feder and Feder (FF) [15]. The FF model is known to rapidly evolve into a state with many well defined avalanches which all recur with the same periodicity. This period of return is completely determined by the sites at the
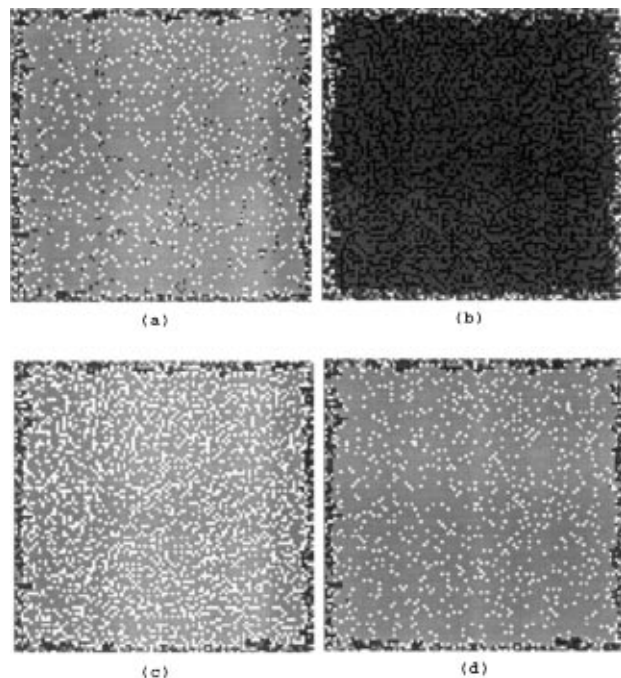

FIG. 4. Snapshots in the time evolution of a 100×100 lattice with the same parameters as in the previous figure. The four figures are in chronological order and the avalanche happens between (a) and (b), while configuration (d) is back to the state shown in (a), after a period T defined in the text. The darker the points, the lower the value of the local function $F_i(t)$.

FIG. 3. Size of avalanches, n, as a function of time for 100×100 lattice in phase II with $\alpha = 0.12$ and $\delta = 0.007$. 10 000 periods T have been rejected. The vertical scale is normalized by the total number of sites on the lattice, N.
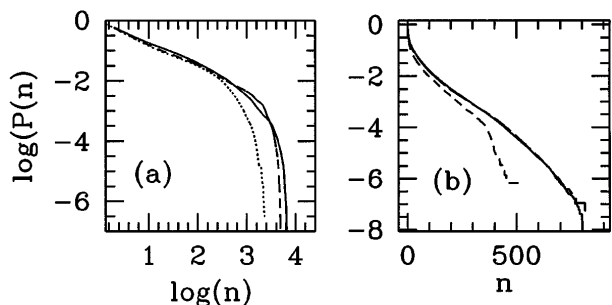
FIG. 5. Integrated probability distribution of avalanches as a function of their size for lattices. (a) Lattice in phase III of the phase diagram (Fig. 1), $\alpha = 0.18$ and $\delta = 0.023$. Lattice sizes are $L = 100$ (dotted line), 169 (dashed line), and 225 (solid line). (b) Lattice in phase IV of the phase diagram, $\alpha = 0.18$ and $\delta = 0.029$. Lattice sizes are $L = 49$ (dashed line), 100 (dotted line), and 169 (continuous line).

edges, which lack a fourth neighbor, giving $P = 1 - 3\alpha$. Nevertheless, for the modified OFC studied here, the factor 3α does not appear in the periodicity of global avalanches. The choice of the dominating avalanche, described previously, is totally controlled by its period of return: It is always the one present with the longest period which wins. If one neglects the presence of the boundary sites in the disordered OFC system, this result can be made consistent with the FF model, where the longer period of $1 - 3\alpha$ is also favored over the bulk period given by $1 - 4\alpha$. The precise value of the return period of the dominating avalanche increases with the disorder, δ, but decreases with α. From observation, the period seems to go as $1 - 4(\alpha - \Delta\delta)$, where $\Delta\delta$ is the width of the disorder distribution from which δ is taken. Many distributions have been tested for the frozen disorder, and all results are consistent with this relation although there is no theoretical argument for this relation.

The results discussed above were obtained on lattices of size $L = 49$, 100, 169, and 225. Size effects vary depending on the phase. In phase I, the size is limited enough to need finite-size scaling. In phases III and IV [see Fig. 5(b)], these effects disappear for size $L = 100$. Effects on the position of the phase boundaries are more difficult to study precisely because of the large numerical effort it would demand. The general trend is the following. For the transition from phase I to phase II, increasing the size decreases the threshold to synchronization, i.e., the larger size, the less quenched disorder it takes to synchronize the lattice. However, it looks as though a finite threshold is needed to destroy the SOC phase for $\alpha > \alpha_d$ even in the very large limit. As for the transition from phase II to phase III, the spatial dimensions of the lattice do not play any noticeable effect in the limit of precision achieved here: Lattices between $L = 49$ and $L = 169$ show transitions for the same values of quenched disorder.

In view of recent discussions about the effect of integrate-and-fire rules versus continuous ones on dynamical systems, results presented here show that the introduction of disorder in an IAF coupled map not only does not destroy the correlations present in the perfect model [1] or simply preserves those already present [3] but increases them in a dramatic fashion. When a finite amount of quenched disorder is applied to the OFC model, the system goes from a self-organized-critical distribution to a single system-wide synchronized and periodic event. On a more general level, the question of the role of disorder in dynamical systems is fundamental because most biological, neurological, or geological dynamical systems evolve in the presence of one or another type of disorder. From the example presented here, it becomes clear that in some cases noise can play a significant part in the synchronization and, therefore, stabilization of cycles in complex systems.

On this model specifically, the exact periodicity of the dominating avalanche as well as the ambiguous role of the boundary sites, isolated but required, remain to be understood. Analytical work on the effects of disorder on coupled systems will also be needed. Above all this, it is important to try to tie these results to experiment on real systems, where disorder and noise are usually found as a matter of fact.

*Present address.

[1] M. Tsodyks, I. Mitkov, and H. Sompolinsky, Phys. Rev. Lett. **71**, 1280 (1993).

[2] P. C. Matthews and S. H. Strogatz, Phys. Rev. Lett. **65**, 1701 (1990).

[3] S. Bottani, Phys. Rev. Lett. **74**, 4189 (1995).

[4] M. I. Dykman, D. G. Luchinsky, R. Mannella, P. V. E. Mc-Clintock, N. D. Stein, and N. G. Stocks, Nuovo Cimento **17D**, 661 (1995).

[5] V. Hakim and W.-J. Rappel, Europhys. Lett. **27**, 637 (1994).

[6] N. Mousseau, J. Phys. A **29**, 3021 (1996).

[7] R. Wackerbauer, Phys. Rev. E **52**, 4745 (1995).

[8] Z. Olami, H. J. S. Feder, and K. Christensen, Phys. Rev. Lett. **68**, 1244 (1992).

[9] A. V. M. Herz and J. J. Hopfield, Phys. Rev. Lett. **75**, 1222 (1995).

[10] P. Grassberger, Phys. Rev. E **49**, 2436 (1994).

[11] A. A. Middleton and C. Tang, Phys. Rev. Lett. **74**, 742 (1995).

[12] I. M. Jánosi and J. Kertész, Physica (Amsterdam) **200A**, 179 (1993).

[13] H. Ceva, Phys. Rev. E **52**, 154 (1995).

[14] N. Mousseau (to be published).

[15] H. J. S. Feder and J. Feder, Phys. Rev. Lett. **66**, 2669 (1991).